Novel Antagonists Acting at the P2Y$_1$ Purinergic Receptor: Synthesis and Conformational Analysis Using Potentiometric and Nuclear Magnetic Resonance Titration Techniques

Pierre Raboisson,[†] Anthony Baurand,[‡] Jean-Pierre Cazenave,[‡] Christian Gachet,[‡] Myriam Retat,[†] Bernard Spiess,*[,†] and Jean-Jacques Bourguignon*[,†]

Laboratoire de Pharmacochimie de la Communication Cellulaire, UMR 7081 du CNRS, Faculté de Pharmacie, Université Louis Pasteur, 74, Route du Rhin, 67401 Illkirch Cedex, France, and Laboratoire de Biologie et de Pharmacologie de l'Hémostase et de la Thrombose, Etablissement Français du Sang-Alsace, U.311 de l'INSERM, 10, Rue Spielmann, BP 36, 67065 Strasbourg Cedex, France

Received August 28, 2001

The human P2Y$_1$ receptor is widely distributed in many tissues and has a classical structure of a G protein-coupled receptor. Activated by adenosine-5′-diphosphate (ADP), this receptor is essential for platelet aggregation. In the present paper, we describe the synthesis of novel P2Y$_1$ antagonists that could be of interest at least as tools to define the physiological roles of the P2Y$_1$ receptor, at best as new antithrombotic agents. Thus, we prepared the 2,N^6-dimethyl-2′-deoxyadenosine-3′,5′-bisphosphate derivative, **1e**. The biological activity was demonstrated by the ability of compound **1e** to inhibit ADP-induced platelet aggregation, shape change, and intracellular calcium rise. This compound was a full antagonist at the P2Y$_1$ receptor with a pA_2 value of 7.11 ± 0.11 and was found to be 4-fold more potent than the reference N^6-methyl-2′-deoxyadenosine-3′,5′-bisphosphate (**1a**, pA_2 = 6.55 ± 0.05), revealing the potency-enhancing effects of the 2-methyl group. The better activity of **1e** as compared to **1a** was analyzed using both potentiometric and nuclear magnetic resonance titration techniques, which highlighted specific conformational features of this compound. These results clearly indicate the preference for both compounds for an anti conformation at the N−glycosyl linkage. Furthermore, the percentage of S conformer of **1e** is close to that of **1a**, which is nearly 70% at pH = 2.8 and increases dramatically when pH increases. From the macroprotonation constants, it can be noted that compound **1e** is significantly more basic than **1a**. This is indeed expected for the N1 adenine nitrogen due to the electron-donating character of the methyl moiety. By considering the microconstants of the phosphate groups, the higher basicity of P3 and P5 for **1e** may be due to the decrease in the local dielectric constant induced by the substitution of the hydrogen atom by a more lipophilic methyl group. Thus, it may be suggested that the gain in activity of **1e** when compared to the reference compound **1a** would result from its gain in basicity rather than steric and conformational modifications. The synthesis of the first selective radioligand acting at the P2Y$_1$ receptor ([^{33}P]-N^6-methyl-2′-deoxyadenosine-3′,5′-bisphosphate, **17**) is also reported and will be used in the future for efficient screening needed for drug optimization.

Introduction

Adenine nucleotides interact with P2 receptors, which are widely distributed in many different cell types including endothelial cells, smooth muscle, epithelial cells, lungs, platelets, the pancreas, and central nervous system and regulate a broad range of physiological processes.[1] These receptors are divided into two families of membrane-bound purinergic receptors. The G protein-coupled or metabotropic receptors are termed P2Y, and the ligand-gated ion channel or ionotropic receptors are termed P2X. It is well-established that a normal platelet response to adenosine-5′-diphosphate (ADP) requires activation of both the P2Y$_1$ receptor, responsible for the mobilization of ionized Ca^{2+} from internal stores, through a Gq phospholipase C pathway and the P2Y$_{12}$ receptor recently identified[2] coupled to Gi and adenylyl cyclase inhibition.[3] The P2Y$_1$ receptor is necessary for ADP to induce platelet aggregation, since its inhibition in vitro by selective antagonists totally abolishes ADP-induced aggregation and calcium mobilization.[3,4] This receptor has been recently shown to be a promising potential target for new antithrombotic drugs.[3] Indeed, P2Y$_1$ null mice display strong resistance to the thromboembolism induced by intravenous injection of a mixture of collagen and adrenaline[5,6] or thromboplastin.[7] Moreover, the administration to mice of the P2Y$_1$ antagonist N^6-methyl-2′-deoxyadenosine-3′,5′-bisphosphate (**1a**) resulted in prolongation of the bleeding time, inhibition of ex vivo platelet aggregation in response to ADP, and resistance to thromboembolism induced by collagen and adrenaline or tissue factor.[7,8]

Thus, selective P2Y$_1$ receptor antagonists may have potential therapeutic use as antithrombotic agents. On the other hand, the exact physiological role of this receptor is largely unknown, and few pharmacological

* To whom correspondence should be addressed. B.S. Tel: +33 390 24 42 23. Fax: 33 390 24 43 10. E-mail: spiess@aspirine.u-strasbg.fr. or J.J.B. Tel: +33 390 24 43 10. Fax: 33 390 24 43 10. E-mail: jjb@pharma.u-strasbg.fr.
† Université Louis Pasteur.
‡ Etablissement Français du Sang-Alsace.

10.1021/jm0104062 CCC: $22.00
Published on Web 01/12/2002

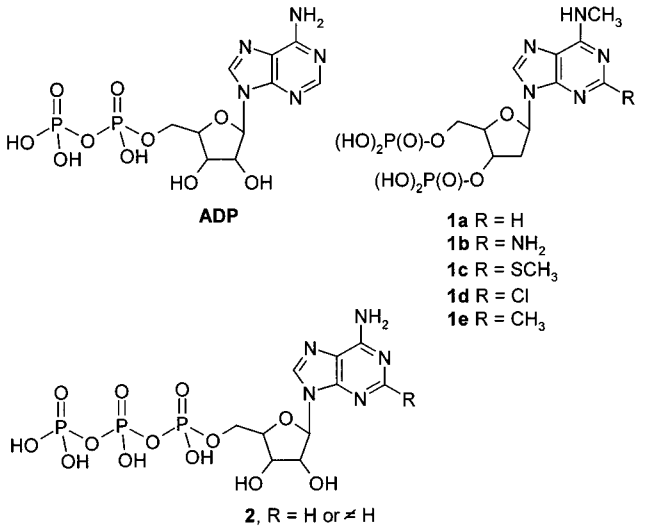

Figure 1. Structures of nucleotides analogues acting on the $P2Y_1$ receptor.

tools are available today. Thus, the development of potent and selective $P2Y_1$ receptor antagonists is of a critical need.

The recently reported adenine nucleotide bisphosphate **1a** (Figure 1)[9] has a K_B value at the human $P2Y_1$ receptor of 100 nM[9] and was inactive at other P2Y receptors subtypes[10,11] including $P2X_2$ and $P2X_4$ receptors.[12] However, the selectivity profile of **1a** for the $P2Y_1$ receptor was not optimized as it displayed significant affinity at $P2X_1$ and $P2X_3$ receptors (IC_{50} = 1.15 and 12.9 μM, respectively).[12]

More recently, 2′-deoxyadenosine bisphosphate derivatives, structurally related to **1a** and presenting various structural modifications at positions 2 and 6 of the adenine ring, have been synthesized with the goal of developing more potent and selective $P2Y_1$ antagonists.[13]

Substitutions at position 2 of adenosine-5′-triphosphate nucleotides (**2**; Figure 1) are known to be tolerated and in some cases are favorable for P2Y receptor agonists.[14] Thus, it is not surprising that the introduction of 2-methylthio and 2-chloro substituents in 2′-deoxyadenosine-3′,5′-bisphosphate led to partial agonists nearly 10 times more potent than the 2-unsubstituted compound.[13] Moreover, the introduction of the N^6-methyl group in these 2-methylthio and 2-chloro derivatives (compound **1c**,**d**; Figure 1) decreased agonist efficacy, affording pure $P2Y_1$ receptor antagonists.[15] On the other hand, major synthetic modifications of the ribose moiety have been carried out to increase biological stability and selectivity for the receptors.[15,16]

However, to our knowledge, the effects of the introduction of an alkyl group at position 2 have not been described. To better understand the structure−activity relationships (SAR) of **1a** structurally related compounds acting to the $P2Y_1$ receptors, the 2-methyl derivative **1e** has been synthesized and tested in vitro in comparison to **1a**.

Its activity at $P2Y_1$ receptors was determined by measuring their capacity to inhibit platelet aggregation in vitro. Furthermore, for further works dealing with drug optimization, the critical need of a radiolabeled ligand of the $P2Y_1$ receptor encouraged us to develop the preparation of [^{33}P]-N^6-methyl-2′-deoxyadenosine-3′,5′-bisphosphate (**17**) for binding experiments. Combining pharmacological data with potentiometric and nuclear magnetic resonance (NMR) analyses allowed us to highlight some conformational and electronic requirements of the ribose bisphosphate moiety as well as of the adenine ring of these adenine derivatives.

Chemical Synthesis

As shown in Scheme 1, 2,N^6-dimethyl-2′-deoxyadenosine (**9**) was prepared by ring fission of the 1,N^6-etheno derivative **4** and subsequent unmasking of the etheno moiety.[17−23]

2′-Deoxyadenosine (**3**) was converted into the 1,N^6-etheno derivative **4** with chloroacetaldehyde according to a previously reported procedure.[17] The presence of the etheno group rendered position 2 of the adenine ring sensitive to nucleophilic attack. Thus, treatment of **4** with aqueous sodium hydroxide[18] afforded the imidazole derivative **5** in 86% yield. Cyclocondensation of **5** with trimethylorthoacetate[18] led to the 2-methyl derivative **6**, which, after treatment with ammonium persulfate phosphate buffer at pH 7.2,[19] afforded the resulting adenine (**7**) in good yield. The reaction of the latter with 1,2-bis[(dimethylamino)methylene]hydrazine[20] in refluxing pyridine[21] afforded the 6-(1,2,4-triazol-4-yl) derivative **8** in 50% yield. Nucleophilic displacement of this triazole moiety in **8** with methylamine[21] led to the corresponding 2,N^6-dimethyl derivative **9**. Finally, phosphorylation of **9** using tetrabenzylpyrophosphate (TBPP),[22,23] followed by catalytic hydrogenation, afforded the expected 2-methyl derivative **1e** in 76% yield.

The radioligand **17** was synthesized as shown in Scheme 2.[24] The N^6-methyl-2′-deoxyadenosine was first reacted with 4,4′-dimethoxytrityl chloride[24] to give the 5′-protected derivative **13**, followed by phosphorylation with TBPP to afford compound **14** in 93% yield.[22,23] Deprotection of the DMT group was achieved by treatment with 90% formic acid for 10 min.[25] The catalytic hydrogenation of compound **15** led to the monophosphorylated compound **16** in 83% yield. Finally, its phosphorylation with ^{33}P was achieved by enzyme-catalyzed trans phosphorylation using polynucleotidase kinase at the Du Pont NEN Laboratory (Le Blanc Mesnil, France).

Biological Activity

Platelet Aggregation. The new derivative **1e** prepared in the present study was first tested as an antagonist in a platelet aggregation assay. The addition of **1e** (20 μM) to washed human platelets took place 30 s before ADP (5 μM) inhibited platelet aggregation and shape change (Figure 2A), while **1e** alone did not induce shape change or aggregation even at high concentrations (up to 100 μM). The nature of inhibition was determined by generating a series of concentration−response curves for ADP in the presence of different concentrations of **1e**. This compound caused a parallel shift to the right of the concentration−response curve, but high concentrations of ADP could completely override high concentrations of **1e** (Figure 2B). Schild analysis of the inhibition gave a pA_2 value of 7.11 ± 0.11 (n = 3) and a slope of 0.66 (Figure 2B inset), which could

Scheme 1. Synthesis of **1e**[a]

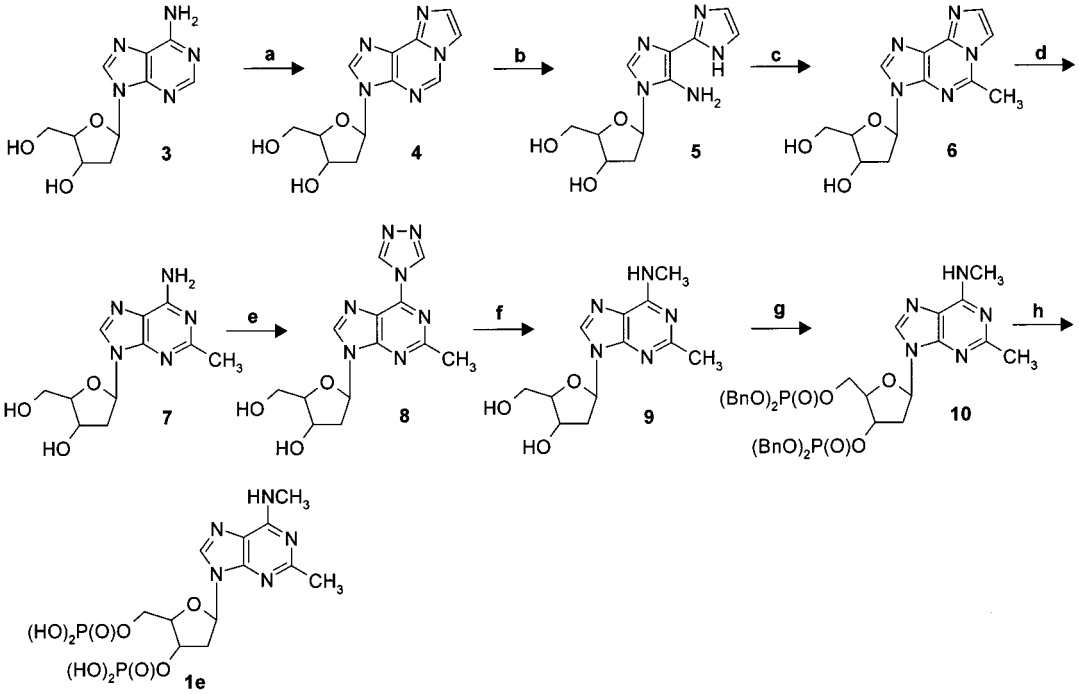

[a] Reagents: (a) $CHOCH_2Cl$; (b) NaOH; (c) $CH_3C(OMe)_3$; (d) $(NH_4)_2S_2O_8$; (e) $(CH_3)_2N{-}N{=}N{-}N(CH_3)_2$; (f) NH_2CH_3; (g) *t*-BuOK, TBPP; (h) H_2, Pd/C.

Scheme 2. Synthesis of **17**[a]

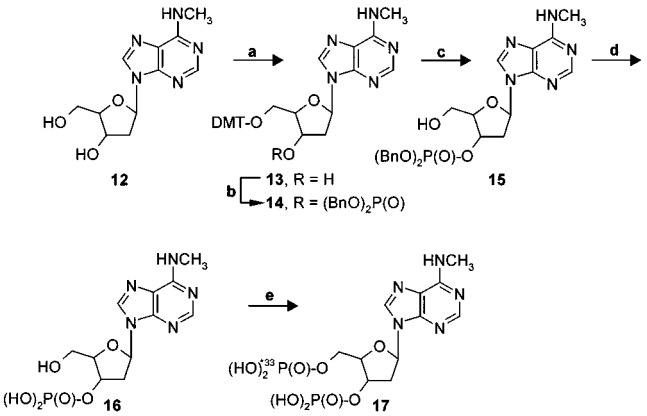

[a] Reagents: (a) DMTCl, DMAP; (b) *t*-BuOK, TBPP; (c) HCOOH; (d) H_2, Pd/C; (e) polynucleotidase kinase.

be explained by the fact that we observed an integrated aggregation process involving the activation of two receptors ($P2Y_1$ and $P2Y_{12}$) and their transduction machinery. Compound **1e** was considerably more potent (about 4-fold) as an antagonist as compared to **1a** ($pA_2 = 6.55 \pm 0.05$).[8] As seen with compound **1a**, no agonist activity was observed.[8] It is interesting to note that the monophosphate derivative **16** was found inactive. This result emphasizes the critical role played by the phosphate in position 5′ of this series of antagonists, in agreement with earlier literature data.[9]

Calcium Mobilization and Inhibition of Adenylyl Cyclase. In platelets, ADP induced simultaneous mobilization of intracellular Ca^{2+} stores and inhibition of adenylyl cyclase, through activation of the $P2Y_1$ and $P2Y_{12}$ receptors, respectively. We have verified that compound **1e** acts selectively on the $P2Y_1$ receptor. The intracellular Ca^{2+} rise induced in washed human platelets by 5 μM ADP could be totally inhibited by 100 μM of **1e**, in the presence or absence of 2 mM external Ca^{2+} (Figure 3A). Conversely, 100 μM of compound **1e** had no influence on basal levels of cyclic adenosine-3′,5′-monophosphate (cAMP) in human platelets (Figure 3B) or on the cAMP levels induced by 10 μM prostaglandin E_1 (PGE_1). The ability of ADP to inhibit PGE_1-stimulated cAMP accumulation was likewise not affected by compound **1e** in human platelets (Figure 3B), whereas AR-C66096,[26] a selective $P2Y_{12}$ receptor antagonist, totally reversed the inhibitory effect of ADP.

Potentiometric Studies and NMR Determinations

Macroscopic and Microscopic Protonation Constants. The studied compounds carry, in addition to a protonable nitrogen on adenine, two phosphate groups, and each group is able to bind only one proton for pH values ranging from 10 to 2.5. Thus, in the latter pH range, three macroscopic overall protonation constants β_y (with $y = 1{-}3$) quantify the protonation process according to the following equilibrium: $L^{4-} + {}_yH^+ \overset{\beta_y}{\rightleftharpoons} H_yL^{(4-y)-}$. When defined step by step, the protonation process may be quantified by K_y, characterizing the equilibrium $H_{y-1}L^{(5-y)-} + H^+ \overset{K_y}{\rightleftharpoons} H_yL^{(4-y)-}$. It can be noted that log K_y corresponds to the usual pK_a value.

These constants, easily determined by potentiometric[27] or NMR titration methods,[28] cannot be attributed to a given protonation site since most of them are less than two log units apart; therefore, a given macroscopic protonation step involves two different basic sites. An inframolecular approach, which aims at defining the intrinsic acid−base properties of each individual functional group, thus requires the resolution of a more detailed protonation scheme, which, in the case of compounds **1e** and **1a**, is depicted in Figure 4.

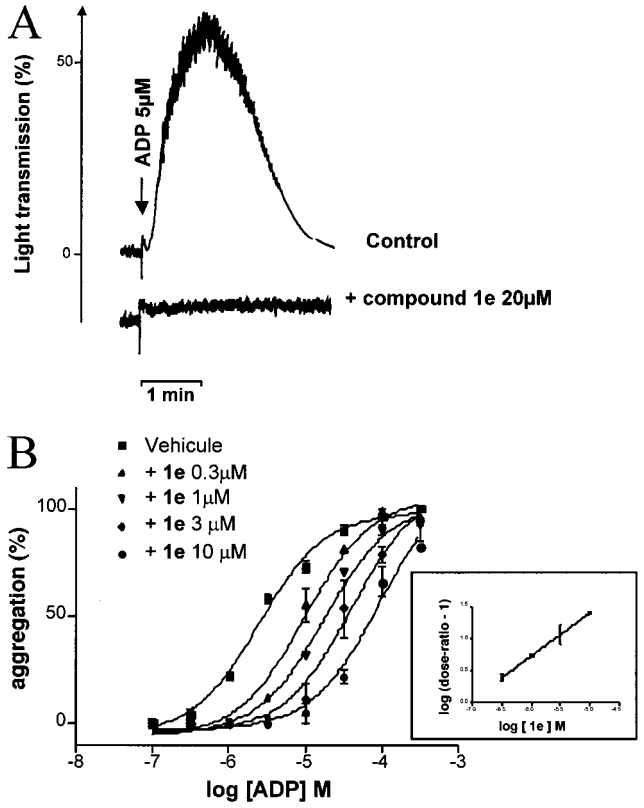

Figure 2. Effect of the compound **1e** on ADP-induced platelet aggregation and shape change. Platelet aggregation was measured as described.[58] The ordinate represents apparent changes in optical density (light transmission) due to the light scattering by the platelets. (A) Aggregation and shape change in response to 5 μM ADP (control) were inhibited by 20 μM of the compound **1e**. Traces are from one experiment representative of three independent experiments giving identical results. (B) Aggregation was induced by increasing concentrations of ADP alone or in the presence of increasing concentrations of the compound **1e** added 30 s before ADP. (Inset) Schild regression analysis of the data shown in panel B. Curves represent the mean of three independent experiments and give a pA_2 value of 7.11 ± 0.11 and a Schild slope of 0.66. Bars show the standard error of mean.

In that figure, the two first protonation steps, which refer to the two phosphate groups, have to be described by four microspecies and four related microprotonation constants. As will be shown later, the third equivalent of added protons mainly binds to an adenine nitrogen, so that K_3 satisfactorily defines the last protonation step.

^{31}P NMR has proven to be a good probe to study individual protonation,[29−40] provided that the observed chemical shifts for the phosphorus resonances δ_i^{obs} mainly depend on the electronic effects accompanying the variations in the protonation states. In that case, the protonated fraction $f_{i,p}$ of a phosphate group in position i on compounds **1e** or **1a** can be calculated by the eq 1:

$$f_{i,p} = \frac{\delta_i^{obs} - \delta_{i,d}}{\delta_{i,p} - \delta_{i,d}} \qquad (1)$$

where $\delta_{i,p}$ and $\delta_{i,d}$ correspond, respectively, to the chemical shifts of the protonated and deprotonated fractions of the phosphates in position i. As previously

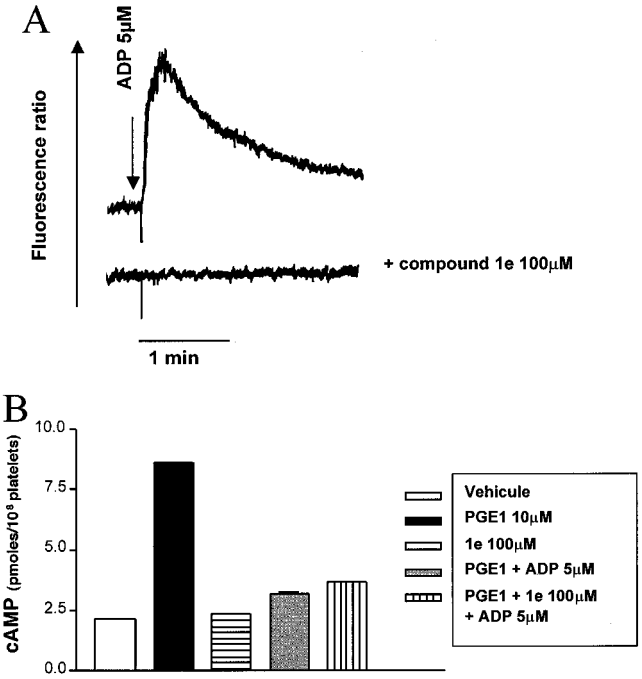

Figure 3. Effects of the compound **1e** on P2Y$_1$ and P2Y$_{12}$ receptor transduction pathways. (A) Added 30 s before ADP, 100 μM compound **1e**, totally abolished the $[Ca^{2+}]_i$ rise induced by 5 μM ADP in washed human platelets in the presence of 2 mM external Ca^{2+}. (B) In the presence of 100 μM compound **1e** (hatched bars), ADP was still able to reduce PGE_1-stimulated cAMP accumulation in washed human platelets. Data are from one experiment representative of three independent experiments giving identical results.

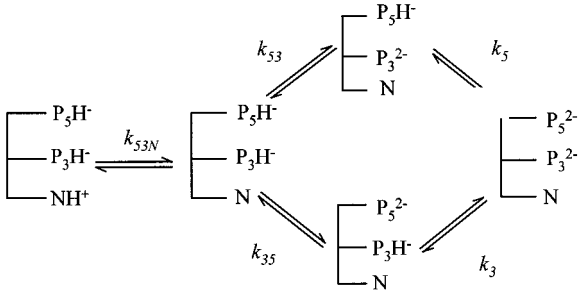

Figure 4. Microscopic protonation scheme for the studied adenosine-3′,5′-bisphosphates.

shown,[35] the individual protonation fractions $f_{i,p}$ may be expressed as a function of the macro- and microprotonation constants

$$f_{i,p} = \frac{\beta_2[H^+]^2 + k_i[H^+]}{\beta_2[H^+]^2 + \beta_1[H^+] + 1} \qquad (2)$$

where k_i refers to k_3 or k_5 of the microequilibria displayed in Figure 4. k_{35} and k_{53} can be further calculated knowing that $K_1K_2 = k_3 \cdot k_{35} = k_5 \cdot k_{53}$. Equation 2 is solved by nonlinear regression introducing the macroprotonation constants obtained by the NMR experiments to give the microprotonation constants.

Results and Discussion

A plot of the chemical shift vs pH for the phosphorus nuclei of **1a** is shown in Figure 5a. The curves for **1e** have the same general shape as those of Figure 5, only they are shifted in their steepest part to higher pH

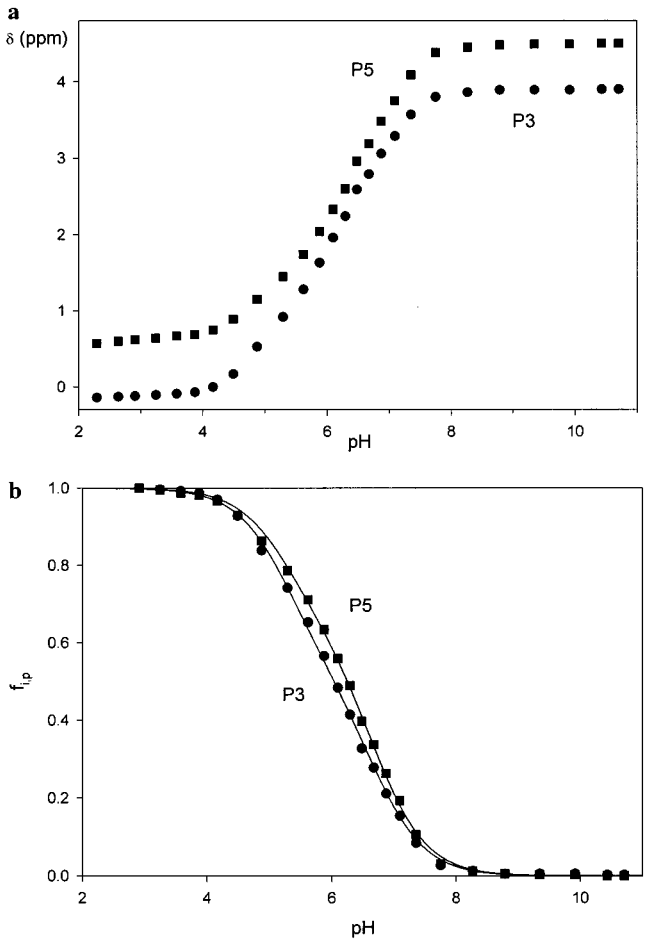

Figure 5. Chemical shifts (δ) from ^{31}P NMR titrations for **1a** (a) and the corresponding protonation fraction curves $f_{i,p}$ (b) as a function of pH in KCl 0.2 M at 37 °C (^2H_2O). The least-squares fit of $f_{i,p}$ vs pH according to type 2 equations is shown in the solid line in panel b.

Table 1.[a]

ligand	y	log β_y	log K_y	i	log k_i	ii'	log $k_{ii'}$
1a	1	6.68	6.68	3	6.40	35	5.55
	2	11.96	5.28	5	6.48	53	5.47
	3	15.87	3.91				
1e	1	7.08	7.08	3	6.76	35	6.26
	2	13.02	5.94	5	6.86	53	6.16
	3	17.69	4.67				

[a] Logarithms of the overall (log β_y) and stepwise macroprotonation constants (log K_y) and microprotonation constants according to Figure 5 for compounds **1a** and **1e**. log k_i and log $k_{ii'}$ represent a general designation for, respectively, the logarithms of the first and second stepwise microprotonation constants. i and ii' allow the location of the protons on the phosphates of the studied compounds. The calculated interactivity parameter $\Delta\log k_{3-5} = \log k_3 - \log k_{53} = \log k_5 - \log k_{35} = 0.93$ for **1a** and 0.60 for **1e**. It can be noted that log K_y also corresponds to the classical pK_a values that refer to a proton dissociation process.

values by about 0.4 pH units. The monophasic shape of these curves indicates only weak interactions between phosphates P3 and P5, each phosphate group having a large conformational freedom. The protonation fraction curves of Figure 5b show, in addition, that both phosphates display about the same basicity, with P5 only slightly more basic than P3. The macro- and microprotonation constants for **1e** and **1a** listed in Table 1 do not only confirm the equivalent basicity of the phosphates for both compounds but also indicate a significant basicity increase of the three functional groups for **1e** with respect to **1a**. By considering the interactivity parameter previously defined,[35] it can be observed that even though they are weak, the interactions between phosphates P3 and P5 are higher for **1e** than for **1a**. Figure 6 shows the distribution of the various microprotonated species as a function of pH, providing a direct observation of the protonation state of the functional groups.

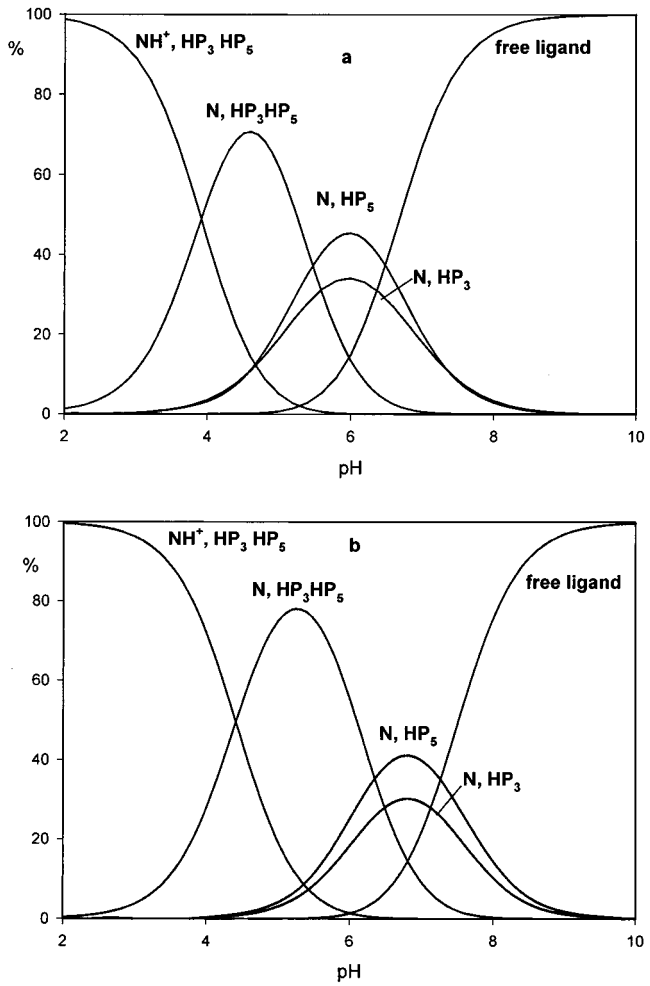

Figure 6. Relative concentrations of the protonated microspecies of compounds **1a** (a) and **1e** (b) in KCl 0.1 M at 37 °C, plotted against pH.

^{1}H NMR titration experiments were performed simultaneously to the ^{31}P NMR titrations in order to gain complementary structural information. The titration curves of Figure 7a,b correspond to the proton resonances of, respectively, compounds **1a** and **1e** that are satisfactorily resolved over the entire studied pH range. Upon protonation, i.e., from pH 11.5 to pH 2.0, it can be seen that most of the protons move significantly downfield (H2, $CH_3$11, H2′, H3′, and H5′ for **1a** and $CH_3$2, $CH_3$11, H2′, H3′, and H5′ for **1e**), some others are only slightly affected (H1′ and H4′), and one of them (H8) undergoes chemical shift variations first to higher fields and then in the opposite direction. It must be recalled that in the most general case, the binding of a proton to a basic site leads to an electron density decrease and thus, via a through bond effect, to a shift of the proton resonances to lower fields. The opposite trend, called "wrongway shift", which has already been

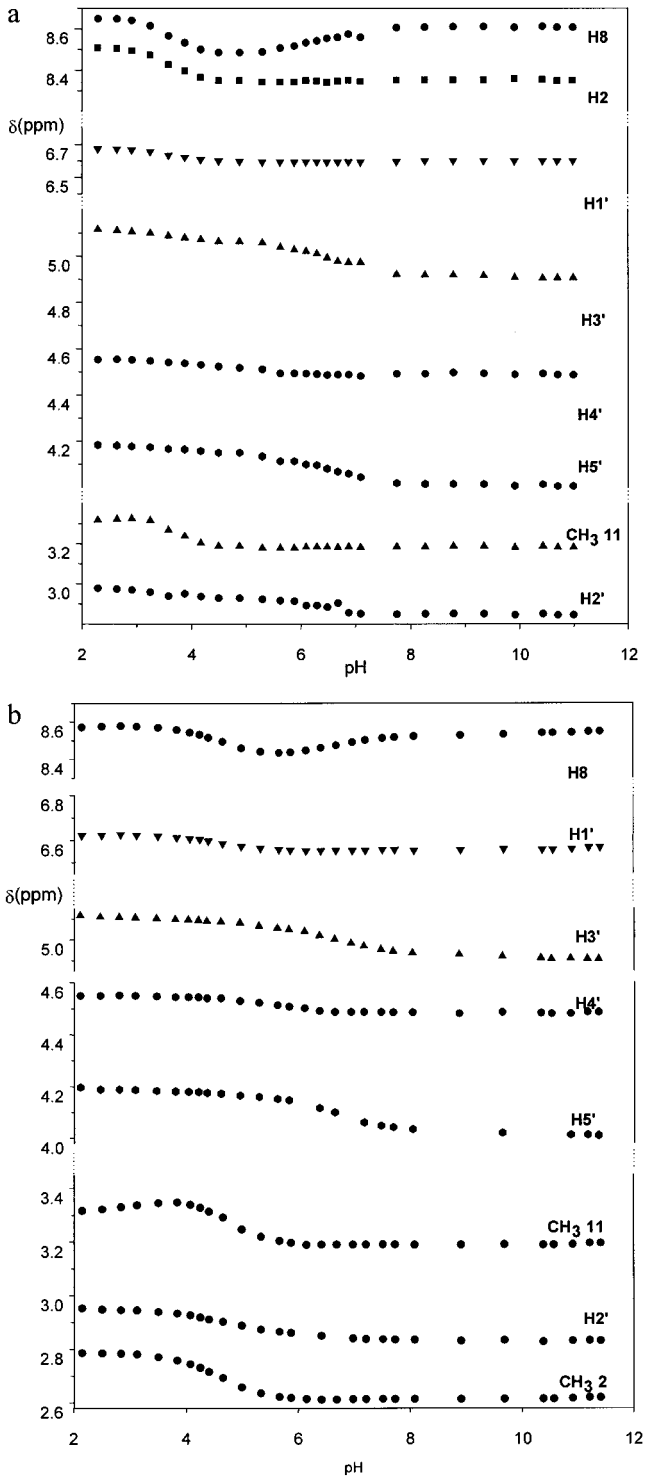

Figure 7. Chemical shifts (δ) from a ^{1}H NMR titration for **1a** (a) and for **1e** (b) as a function of pH in 0.2 M KCl at 37 °C (^2H_2O).

observed in nucleotides,[41−45] inositol-phosphates,[29,46] and natural compounds such as adenophostin A,[30] occurs when a highly negatively charged phosphate group approaches a hydrogen atom. This effect, electrostatic in origin, operates through the field[29,43,44] and affects the chemical shifts of the hydrogen atoms in the neighborhood of the phosphate groups, thus providing valuable structural and conformational information.

From the curves in Figure 7a,b, it can be seen that H2 or $CH_3$2, H8, and $CH_3$11 are sensitive to the protonation occurring at the N1 adenine nitrogen since the electron density changes at this site can be easily transmitted through the π system of the aromatic ring to more distant places. This has been described earlier about many adenine derivatives.[43,44] Also, expected downfield shifts of about 0.16 ppm arise for H3′ and H5′, centered around pH 6.5, which corresponds to the inflection point of P3 and P5. This clearly results from the electron-withdrawing effect of both phosphates on H3′ and H5′. Although less important, the same effect operates on the phosphate remote H2′ and H4′ protons. Finally, the wrongway shift of H8 attests the electrostatic field effect experienced by this proton when protonation of the phosphate groups occurs. This clearly shows the preference for both compounds for an anti conformation at the N−glycosyl bond. A recently published work on C2- or C8-modified nucleotides[47] also concluded that there was a preferential anti conformation for the 2-substituted derivatives and a syn conformation for most of the 8-substituted nucleotides due to steric hindrance. These observations further lead to the conclusions that anti type nucleotides are needed to tightly fit the binding cavity of the $P2Y_1$ receptor. Regarding the anti- or syn-N−glycoside conformational requirements, our results are fully in line with those of literature reports.[16,47]

However, in addition to the orientation at the N−glycosyl bond, the two-state conformational equilibrium of the pentofuranosyl moiety of the compounds under study must also be considered in order to further delineate the steric and conformational demands for optimal binding in the $P2Y_1$ receptor cleft. NMR studies on nucleosides and nucleotides showed that north (N) ($C_{3'}$-*endo*-$C_{2'}$-*exo*) and south (S) ($C_{2'}$-*endo*-$C_{3'}$-*exo*) conformations are the dominant forms in the two-state pseudorotational equilibrium (N ↔ S) in solution.[48−51] The pseudorotational parameters and percentage populations N and S can be accurately calculated from the proton−proton coupling constants for the ribose moiety by using a generalized Karplus equation.[52,53] However, in a simpler approach,[54,55] the percentage of N and S type conformers may be obtained from $^3J_{1',2'}$ and $^3J_{3',4'}$ by the following equation: $S(\%) = [^3J_{1',2'}/(^3J_{1',2'} + {}^3J_{3',4'})] \times 100$, where the sum of $^3J_{1',2'}$ and $^3J_{3',4'}$ should be nearly 10 Hz. The H−H coupling constants of compound **1e** at pH 2.8 were as follows: $^3J_{1',2'} = {}^3J_{1',2''} = 6.8$ Hz, $^3J_{2',2''} = 14.1$ Hz, $^3J_{2',3'} = 5.6$ Hz, $^3J_{2'',3'} = 2.7$ Hz, $^3J_{3',4'} = 2.8$ Hz, and $^3J_{4',5'} = 3.6$ Hz. Thus, the percentage of the S conformer of **1e** is calculated to be nearly 70%. The coupling constants of **1a** are close to those of **1e**, so that about the same percentage of S conformer can be calculated for both compounds. These results are in good agreement with those published for 3′-AMP and 3′-2′-deoxyAMP,[56] which take up, at 278 K, respectively, a 74 and 76% S type conformation.

Interestingly, by increasing pH, the coupling constants slightly vary. Thus, for instance, $^3J_{1',2'}$ and $^3J_{1',2''}$ differentiate from pH 4.5 to pH 9.5: the former increases by ca. 1 Hz, and the latter decreases by ca. 0.5 Hz. For the highest pH values, $^3J_{1',2'}$ reaches 8 Hz, which corresponds to the limiting values for the S conformer.[50] In other words, the percentage of S conformer increases when pH increases. An inspection of a simple molecular model shows that the S conformation of the ribose

moiety ensures a minimal repulsion between the P3 and the P5 phosphates groups and that the repulsion increase expected with the deprotonation of these phosphates drives the sugar pseudorotational equilibrium to the S conformer.

In a recently published paper,[16] molecular modeling studies were carried out in order to analyze the sugar conformational requirements for bisphosphate ligands, among them **1a**, for optimal binding to the human $P2Y_1$ receptor. From these studies, the N conformation appeared to be essential to maximize the electrostatic interactions between the negatively charged phosphate groups and the positively charged amino acids (Arg128-(TM3), Lys280(TM6), and Arg310(TM7)) present in the receptor binding cleft. Because only one pseudorotational form is expected to be present at the binding site of the receptor, the formation of the ligand−receptor complex would require a conformational flip from S to N of high energetic cost, which is likely to be detrimental to optimal binding. If undoubtedly in our experimental conditions the S conformer largely predominates, it is well-known that in solution, various steric and stereoelectronic effects of the sugar skeleton and the nucleobase dictate the N ↔ S pseudorotational equilibrium. It is, therefore, also possible that in biological conditions, factors such as the dielectric constant of the medium and the presence in the neighboring environment of these polyfunctional ligands of inorganic (Ca^{2+}, Mg^{2+}, K^+ ...) or organic (spermine, spermidine ...) cations may greatly influence the conformational properties of the studied adenosine-3′,5′-bisphosphates.

In light of the physicochemical properties of both compounds, what could be the reasons for the higher affinity of **1e** with regard to **1a** for the $P2Y_1$ receptor? From the macroprotonation constants, it can be noted that compound **1e** is significantly more basic than **1a**. This is indeed expected for the N1 adenine nitrogen due to the electron-donating character of the methyl moiety, which could maximize the hydrogen-bonding interaction between the N6 amine of the adenine moiety and the Gln307(TM7) and/or Ser314(TM7) present within the binding site. However, by considering the microconstants of the phosphate groups, the higher basicity of P3 and P5 for **1e** is much more surprising since the inductive electronic effect previously evoked can no longer apply for these remote phosphate groups. Our hypothesis is that the observed basicity increase at least partly stems from the decrease in the local dielectric constant induced by the substitution of a hydrogen atom by a more lipophilic methyl group. Because it has been shown that the affinity of phosphate groups for various polyamines increases by increasing their basicity, it may be suggested that the gain in the receptor affinity of **1e** with regard to **1a** partially reflects its gain in basicity. We also hypothesize that the enhanced affinity reported for the 2-methylthio **1c** or chloro **1d** derivatives[16] may be attributed to the same effect. For the latter, for instance, the withdrawing electron effect of the chlorine atom may lower the basicity of the adenine nitrogen but because it is as lipophilic as the methyl group, it may increase the basicity of the phosphate groups. Moreover, it was not surprising that the more hydrophilic 2-NH_2 derivative was less active as the 2-chloro, 2-methyl, and 2-thiomethyl ones.[16] Even though the lipophilic character of the substituents accounts for the observed biological results, other effects such as changes in the H-bonding pattern of the adenyl moiety cannot be disregarded.

In summary, we have synthesized and evaluated the 2,N^6-dimethyl-2′-deoxyadenosine-3′,5′-bisphosphate derivative, **1e**. The chosen chemical pathway allowed us to explore in a very expeditive way different substitutions at position 2 by means of the corresponding ortho ester and by using the amino-imidazol as a common intermediate leading to possible topological exploration at this position. The 2-methyl derivative (**1e**) was tested as an antagonist of platelet aggregation. At the intracellular level, as expected for a $P2Y_1$ receptor antagonist, compound **1e** totally inhibited the intracellular Ca^{2+} mobilization induced by ADP but had no effect on its inhibition of adenylyl cyclase. Thus, compound **1e** was significantly more potent (about 4-fold) as an antagonist as compared to **1a** ($pA_2 = 6.55 \pm 0.05$),[8] revealing the potency-enhancing effects of the 2-methyl group. As seen with compound **1a**, no agonist activity was observed.[8]

To better understand the SAR of **1a** structurally related compounds acting on the $P2Y_1$ receptor, we have used an integrated approach combining NMR and potentiometric titration experiments, which led to the following observations: (i) both compounds **1a** and **1e** possess an anti conformation at the N−glycosyl linkage, and the percentage of S conformer of **1e** is close to that of **1a**, nearly 70% at pH 2.8 and increasing dramatically when pH increases; (ii) from the macroprotonation constants, it can be noted that compound **1e** is significantly more basic than **1a** at the N1 adenine nitrogen, due to the electron-donating character of the methyl moiety; (iii) by considering the microconstants of the phosphate groups, the higher basicity of P3 and P5 for **1e** may be due to the decrease in the local dielectric constant induced by the substitution of a hydrogen atom by a more lipophilic methyl group. Thus, it may be suggested that the gain in receptor affinity of **1e** with regard to **1a** also reflects its gain in basicity rather than steric and conformational modifications.

The synthesis of the radiolabeled ligand of the $P2Y_1$ receptor **17** has also been reported. As previously described,[8] this compound is now readily available for further binding studies.

Experimental Section

Chemical Synthesis. Reagents used for the synthesis were purchased from Sigma-Aldrich (Isle d'Abeau Chesnes, France) and Lancaster (Bischheim-Strasbourg, France). With the exception of tetrahydrofuran (THF) and Et_2O, all solvents were obtained from commercial suppliers and used without further purification. These two solvents were freshly distilled from sodium benzophenone ketyl. Flash chromatography was performed on Geduran silica gel Si 60 (40−63 μm, Merck). Thin-layer chromatography was carried out using plates of silica gel 60 F_{254} (Merck). The spots were visualized either under UV light ($\lambda = 254$ nm) or by spraying with molybdate reagent (H_2O/concentrated H_2SO_4/$(NH_4)_6Mo_7O_{24}\cdot 4H_2O$/$(NH_4)_2$-$Ce(SO_4)_4\cdot 2H_2O$, 90/10/25/1, v/v/w/w) and charring at 140 °C for a few minutes. All chemical yields are unoptimized and generally represent the result of a single experiment.

^{1}H NMR were recorded on a Bruker AC 200 (200 MHz) or a Bruker DPX 300 (300 MHz) spectrophotometer at room temperature. Chemical shifts are given in parts per million (δ), coupling constants (J) are in hertz (Hz), and signals are

designated as follows: s, singlet; d, doublet; t, triplet; q, quadruplet; quint, quintuplet; m, multiplet; br s, broad singlet; etc. The mass spectra were obtained on a Mariner API-TOF.

Melting points were determined with a Mettler FP62 apparatus and are uncorrected. Elemental analyses were performed by the CNRS department of microanalysis (CNRS, Vernaison, France) and are indicated only by the elemental symbols within ±0.4% of the theoretical values unless otherwise noted.

2-Methyl-2′-deoxyadenosine (7). To a solution of **3** (835 mg, 3.10 mmol) in H_2O (30 mL) and THF (30 mL) was added a 50% solution of chloroacetaldehyde in water (6,50 mL, 51.2 mmol) at 20 °C with stirring, and the pH was maintained at 4−5 with saturated $NaHCO_3$. After the solution was stirred for 4 days at 20 °C, the solvent was evaporated to dryness and the residue was purified on silica gel (CH_2Cl_2/AcOEt/EtOH, 50:40:10) to give a white solid, which was recrystallized from EtOH and Et_2O to give **4** (735 mg, 83%) as a white solid. ^{1}H NMR (200 MHz, $CDCl_3$): δ 2.33−2.44 (m, 1H, 2′-Ha), 2.53−2.83 (m, 1H, 2′-Hb), 3.51−3.71 (m, 2H, 5′-H), 3.88−3.95 (m, 1H, 4′-H), 4.41−4.48 (m, 1H, 3′-H), 5.02 (t, 1H, J = 5.7 Hz, 3′-OH), 5.41 (d, 1H, J = 3.90 Hz, 5′-OH), 6.47−6.53 (m, 1H, 1′-H), 7.58 (d, 1H, J = 0.84 Hz, etheno Ha), 8.10 (d, 1H, J = 0.84 Hz, etheno Hb), 8.56 (s, 1H, 8-H), 9.31 (s, 1H, 2-H); *m*/*z* 276 $(M + H)^+$.

A solution of **4** (1.00 g, 3.63 mmol) in 0.5 N NaOH (50 mL) was stirred under reflux for 2 min and then cooled to room temperature. The solution was neutralized with 1 N HCl. The mixture was evaporated to dryness. The residue was triturated in EtOH (150 mL) and then filtered and washed with EtOH. The combined filtrates were evaporated to dryness, and the residue was redissolved in EtOH (7 mL). To this solution was added 1 mL of Et_2O. The mixture was stirred at room temperature for 0.5 h. The precipitate was filtered, washed with Et_2O, and then recrystallized from EtOH and Et_2O to yield **5** (830 mg, 86%) as a white powder. ^{1}H NMR (200 MHz, dimethyl sulfoxide (DMSO)-d_6 + D_2O): δ 2.11−2.19 (m, 1H, 2′-Ha), 2.41−2.51 (m, 1H, 2′-Hb), 3.50−3.55 (m, 2H, 5′-H), 3.78−3.82 (m, 1H, 4′-H), 4.31−4.35 (m, 1H, 3′-H), 5.92−5.98 (m, 1H, 1′-H), 6.87 (s, 2H, etheno H), 7.40 (s, 1H, 2-H); *m*/*z* 266 $(M + H)^+$.

A mixture of **5** (300 mg, 1.13 mmol), trimethylorthoacetate (2.16 mL, 17 mmol), trifluoroacetic acid (200 μL, 2.60 mmol), and anhydrous dimethylformamide was heated at 100 °C overnight under an argon atmosphere and then concentrated to dryness. The residue was purified on silica gel (AcOH/MeOH/CH_2Cl_2, 5:20:75) to give a white solid, which was recrystallized from EtOH and Et_2O to give **6** (265 mg, 81%) as a white solid. ^{1}H NMR (200 MHz, DMSO-d_6): δ 2.31−2.42 (m, 1H, 2′-Ha), 2.68−2.82 (m, 1H, 2′-Hb), 2.88 (s, 3H, CH_3), 3.53−3.70 (m, 2H, 5′-H), 3.89−3.94 (m, 1H, 4′-H), 4.40−4.50 (m, 1H, 3′-H), 5.02 (t, 1H, J = 5.4 Hz, 3′-OH), 5.37 (d, 1H, J = 3.2 Hz, 5′-OH), 6.50 (t, 1H, J = 6.7 Hz, 1′-H), 7.61 (d, 1H, J = 1.5 Hz, etheno Ha), 8.01 (d, 1H, J = 1.5 Hz, etheno Hb), 8.49 (s, 1H, 8-H); *m*/*z* 312 $(M + Na)^+$.

To a stirred solution of $(NH_4)_2S_2O_8$ (433 mg, 1.90 mmol) in 0.5 M phosphate buffer, pH 7.5, at room temperature was added **6** (250 mg, 0.864 mmol). The mixture was heated at 80 °C for 1 h and then evaporated. The residue was triturated in EtOH (100 mL) and then filtered and washed with EtOH. The combined filtrates were evaporated to dryness, and the residue was chromatographed on silica AcOH/MeOH/CH_2Cl_2, 5:20:75) to give a white solid, which was recrystallized from EtOH and Et_2O to give **7** (138 mg, 60%) as a white solid. ^{1}H NMR (200 MHz, DMSO-d_6): δ 2.18−2.28 (m, 1H, 2′-Ha), 2.40 (s, 3H, CH_3), 2.61−2.79 (m, 1H, 2′-Hb), 3.50−3.70 (m, 2H, 5′-H), 3.90−3.93 (m, 1H, 4′-H), 4.39−4.52 (m, 1H, 3′-H), 5.34 (t, 1H, J = 5.4 Hz, 3′-OH), 5.59 (d, 1H, J = 3.2 Hz, 5′-OH), 6.33 (t, 1H, J = 7.09 Hz, 1′-H), 7.26 (s, 2H, NH_2), 8.26 (s, 1H, 8-H); *m*/*z* 266 $(M + H)^+$. Anal. ($C_{11}H_{15}N_5O_3$·$1H_2O$) C, H, N.

2,N^6-Dimethyl-2′-deoxyadenosine (9). A mixture of dried **7** (250 mg, 0.94 mmol) and 1,2-bis[(dimethylamino)methylene]-hydrazine (535 mg, 3.76 mmol) in anhydrous pyridine (3 mL) was evaporated to dryness and then dried under vacuum for 30 min. The residue was dissolved in anhydrous pyridine (5 mL). The resulting solution was cooled to 0 °C, and thenm TMSCl (235 μL, 1.85 mmol) was added. The mixture was heated at 100 °C under argon for 24 h and cooled to 0 °C, and then, additional TMSCl (94 μL, 0.74 mmol) was added. After the solution was stirred for 15 min at 20 °C, the solvent was evaporated to dryness and the residue was dissolved in ice-cold CH_2Cl_2 (80 mL). This solution was successively washed with a cold mixture of brine (40 mL) and saturated $NaHCO_3$ (20 mL), brine (40 mL) and 1 N HCl (15 mL), and finally with water (20 mL). The organic layer was dried (Na_2SO_4) and concentrated under reduced pressure. The residue was dissolved in absolute MeOH (15 mL), and the resulting solution was stirred at room temperature overnight. The solvent was evaporated, and a mixture of CH_2Cl_2 (8 mL) and MeOH (1 mL) was added. The precipitate was filtered, washed with CH_2Cl_2, and then dried in vacuo to give **8** (149 mg, 50%) as a white solid. ^{1}H NMR (200 MHz, DMSO-d_6): δ 2.34−2.46 (m, 1H, 2′-Ha), 2.72−2.85 (m, 1H, 2′-Hb), 2.77 (s, 3H, CH_3), 3.53−3.71 (m, 2H, 5′-H), 3.90−3.97 (m, 1H, 4′-H), 4.43−4.51 (m, 1H, 3′-H), 5.07 (s, 1H, 3′-OH), 5.42 (s, 1H, 5′-OH), 6.52 (t, 1H, J = 6.6 Hz, 1′-H), 8.93 (s, 1H, 8-H), 9.62 (s, 2H, triazole); *m*/*z* 318 $(M + H)^+$.

A solution of **8** (150 mg, 0.472 mmol) and methylamine (1.0 M in THF, 3 mL) in absolute ethanol (3 mL) was heated at 100 °C in a sealed tube for 12 h. After the solvent was evaporated, the residue was chromatographed on silica (AcOEt/CH_2Cl_2/EtOH, 4:5:1) and then recrystallized from ethanol to give **9** (118 mg, 90%) as a white solid; mp 150 °C. ^{1}H NMR (200 MHz, $CDCl_3$): δ 2.26−2.36 (m, 1H, 2′-Ha), 2.61 (s, 3H, CH_3), 3.10−3.25 (m, 1H, 2′-Hb), 3.24 (m, 3H, CH_3), 3.78−4.09 (m, 2H, 5′-H), 4.28−4.31 (m, 1H, 4′-H), 4.82−4.89 (m, 1H, 3′-H), 5.98 (s, 1H, NH), 6.29−6.37 (m, 1H, 1′-H), 7.74 (s, 1H, 3′-OH), 8.25 (s, 2H, 8-H, 5′-OH); *m*/*z* 280 $(M + H)^+$. Anal. ($C_{12}H_{17}N_5O_3$·0.5 H_2O) C, H, N.

***2,N*^{6}-Dimethyl-2′-deoxyadenosine-3′,5′-bisphosphate (1e).** Potassium *tert*-butoxide (1.0 M in THF, 1.10 mL) was slowly added, at −40 °C, to a stirred solution of **9** (140 mg, 0.50 mmol) in anhydrous THF (10 mL). After 5 min, tetrabenzyl pyrophosphate (592 mg, 1.10 mmol) was added and stirring was continued for 15 min at −40 °C. The reaction mixture was allowed to warm to 0 °C and was then quenched with acetic acid (50 μL). The mixture was diluted with ethyl acetate, washed with water, dried (Na_2SO_4), and concentrated to dryness under reduced pressure. Chromatography on silica (AcOEt/CH_2Cl_2/EtOH, 40:50:10) afforded the desired product **10** (264 mg, 66%) as a colorless syrup. ^{1}H NMR (200 MHz, $CDCl_3$): δ 2.40−2.52 (m, 1H, 2′-Ha), 2.57−2.77 (m, 1H, 2′-Hb), 2.60 (s, 3H, CH_3), 3.23 (d, 3H, J = 4.0, NCH_3), 4.08−4.29 (m, 3H, 5′-H, 4′-H), 4.98−5.12 (m, 9H, 3′-H, 4CH_2), 5.72 (m, 1H, NH), 6.28−6.36 (m, 1H, 1′-H), 7.29−7.38 (m, 20H, 4Ph), 8.23 (s, 1H, 8-H); *m*/*z* 800 $(M + H)^+$.

A mixture of **10** (120 mg, 0.15 mmol) and 10% Pd/C (100 mg) in absolute methanol (20 mL) was shaken in a hydrogenation apparatus under atmosphere pressure at room temperature for 48 h. The catalyst was removed by filtration and washed with water, and the filtrate was concentrated to dryness. Recrystallization from methanol yielded compound **1e** (50 mg, 76%) as a colorless solid; mp 146 °C. ^{1}H NMR (200 MHz, DMSO-d_6): δ 2.44 (s, 3H, CH_3), 2.50−2.65 (m, 1H, 2′-Ha), 2.80−2.90 (m, 1H, 2′-Hb), 2.94 (m, 3H, CH_3), 3.95−4.12 (m, 2H, 5′-H), 4.22−4.35 (m, 1H, 4′-H), 4.93−5.04 (m, 1H, 3′-H), 6.36 (t, 1H, J = 4.5, 1′-H), 7.72 (s, 1H, NH), 8.25 (s, 1H, 8-H). ^{31}P NMR (300 MHz, D_2O): δ 2.74 (s, 1P, 3-P), 3.10 (s, 1P, 5-P). Anal. ($C_{12}H_{19}N_5O_9P_2$·$0.2H_2O$) C, H, N.

***N*^{6}-Methyl-2′-deoxyadenosine-3′-phosphate (16).** Compound **12**[57] (400 mg, 1.51 mmol) was dissolved in pyridine (10 mL) and then evaporated to dryness. This operation was repeated twice, and then, the residue was suspended in dry pyridine (10 mL) under an argon atmosphere. 4,4′-Dimethoxytrityl chloride (511 mg, 1.51 mmol), triethylamine (210 μL, 1.51 mmol), and 4-(dimethylamino)pyridine (10 mg, 0.0819 mmol) were then added, and the resulting solution was stirred for 6 h at room temperature. After the solvents were evaporated,

the residue was diluted with ethyl acetate, washed with cold water (20 mL) and saturated sodium bicarbonate (10 mL), dried (Na_2SO_4), and concentrated to dryness under reduced pressure. Chromatography on silica (CH_2Cl_2/MeOH, 80:20) afforded compound **13** (668 mg, 78%) as a colorless solid. ^{1}H NMR (300 MHz, $CDCl_3$): δ 2.49−2.57 (m, 1H, 2′-Ha), 2.79−2.88 (m, 1H, 2′-Hb), 3.20 (d, 3H, J = 4.1, NCH_3), 3.37−3.45 (m, 2H, 5′-H), 3.78 (s, 6H, $2OCH_3$), 4.11−4.15 (m, 1H, 4′-H), 4.64−4.73 (m, 1H, 3′-H), 5.73 (q, 1H, J = 4.1, NH), 6.44 (t, 1H, J = 6.4, 1′-H), 6.78−6.85 (m, 4H, 4CH), 7.21−7.45 (m, 9H, 9CH), 7.89 (s, 1H, 2-H), 8.35 (s, 1H, 8-H); m/z 590 $(M + Na)^+$.

Prepared from **13** (65 mg, 0.115 mmol), potassium *tert*-butoxide (1.0 M in THF, 126 μL), and tetrabenzyl pyrophosphate (68 mg, 0.126 mmol) using the procedure described for compound **10**, compound **14** (89 mg, 93%) was obtained as a hygroscopic colorless solid. ^{1}H NMR (200 MHz, $CDCl_3$): δ 2.57−2.67 (m, 1H, 2′-Ha), 2.87−3.01 (m, 1H, 2′-Hb), 3.23 (d, 3H, J = 4.9, NCH_3), 3.27−3.70 (m, 2H, 5′-H), 3.80 (s, 6H, $2OCH_3$), 4.29−4.34 (m, 1H, 4′-H), 5.04−5.10 (m, 4H, $2CH_2$), 5.14−5.29 (m, 1H, 3′-H), 5.72 (q, 1H, J = 4.9, NH), 6.36 (m, 1H, 1′-H), 6.76−6.83 (m, 4H, 4CH), 7.23−7.42 (m, 19H, 19CH), 7.84 (s, 1H, 2-H), 8.35 (s, 1H, 8-H); m/z 828 $(M + H)^+$.

A stirred solution of **14** (600 mg, 0.73 mmol) in CH_2Cl_2 (5 mL) was treated with formic acid (5 mL) at room temperature for 1 h. After the yellow mixture was concentrated, the residue was redissolved in ethyl acetate (20 mL), washed with dilute sodium bicarbonate, and dried over Na_2SO_4. Removal of the solvent in vacuo afforded a residue, which was purified by silica gel column chromatography (AcOEt/CH_2Cl_2/EtOH, 40:50:10) to give compound **15** (372 mg, 97%) as a colorless solid. ^{1}H NMR (300 MHz, $CDCl_3$): δ 2.33−2.39 (m, 1H, 2′-Ha), 2.97−3.10 (m, 1H, 2′-Hb), 3.18 (br s, 3H, NCH_3), 3.58−3.87 (m, 2H, 5′-H), 4.23−4.25 (m, 1H, 4′-H), 5.04−5.19 (m, 5H, 3′-H, $2CH_2$), 6.04−6.08 (m, 1H, 1′-H), 7.18 (br s, 1H, NH), 7.30−7.45 (m, 10H, 10CH), 7.76 (s, 1H, 2-H), 8.36 (s, 1H, 8-H); m/z 526 $(M + H)^+$.

A mixture of **15** (130 mg, 0.247 mmol) and 10% Pd/C (100 mg) in absolute methanol (20 mL) was shaken in a hydrogenation apparatus at room temperature for 24 h. The catalyst was removed by filtration and washed with water, and the filtrate was concentrated to dryness. Recrystallization from methanol and diethyl ether yielded **16** (71 mg, 83%) as a colorless solid; mp 167 °C. ^{1}H NMR (300 MHz, DMSO-d_6): δ 2.51−2.57 (m, 1H, 2′-Ha), 2.83−2.93 (m, 1H, 2′-Hb), 2.94 (br s, 3H, CH_3), 3.53−3.68 (m, 2H, 5′-H), 4.12−4.16 (m, 1H, 4′-H), 4.90−4.95 (m, 1H, 3′-H), 6.33−6.38 (m, 1H, 1′-H), 7.87 (br s, 1H, NH), 8.28 (s, 1H, 2-H), 8.34 (s, 1H, 2-H). Anal. ($C_{11}H_{16}N_5O_6P\cdot0.5H_2O$) C, H, N.

Biological Tests. ADP and PGE_1 were from Sigma (Saint Quentin-Fallavier, France). Human fibrinogen was from Kabi (Stockholm, Sweden), fura-2/acetoxymethyl ester (fura-2/AM) was from Calbiochem (Meudon, France), and the cAMP assay kit was from Amersham (Les Ulis, France). Apyrase was purified from potatoes as previously described.[58] Compound **1a** was synthesized by P. Raboisson (CNRS, Faculty of Pharmacy, Strasbourg, France).[13]

Washed Human Platelet Aggregation. Washed human platelets were prepared as previously described[58] and resuspended at 3×10^5 platelets/μL in Tyrode's buffer containing 2 mM $CaCl_2$, in the presence of 0.02 U/mL of the ADP scavenger apyrase (adenosine 5′-triphosphate diphosphorylase, EC 3.6.1.5). Platelets were kept at 37 °C throughout all experiments, and aggregation was measured by standard methods.[58]

Briefly, a 450 μL aliquot of platelet suspension was stirred at 1100 rpm and activated by the addition of agonists and human fibrinogen (0.8 mg/mL), in a final volume of 500 μL. The extent of aggregation was estimated quantitatively by measuring the maximum curve height above the baseline.

$[Ca^{2+}]_i$ Measurements. Fura-2/AM-loaded human platelets were prepared as previously described[4] and resuspended in Tyrode's buffer with 2 mM $CaCl_2$. Aliquots of fura-2-loaded platelets were transferred to a 10 mm × 10 mm quartz cuvette maintained at 37 °C and fluorescence measurements were performed under continuous stirring, in a PTI Deltascan spectrofluorimeter (Photon Technology International Inc., Princetown, NJ).[4] The excitation wavelength was alternately fixed at 340 or 380 nm, fluorescence emission was determined at 510 nm, and results were calculated as the fluorescence ratio (340/380) in arbitrary units.

Measurement of Adenylyl Cyclase Activity. A 450 μL aliquot of washed platelets resuspended in Tyrode's buffer containing 2 mM Ca^{2+} and 1 mM Mg^{2+} was stirred at 1100 rpm in an aggregometer cuvette, and the following reagents were added at 30 s intervals: (i) 10 μM PGE_1, (ii) 100 μM compound **1e**, and (iii) 5 μM ADP or vehicle (Tyrode's buffer containing no Ca^{2+} or Mg^{2+}). The reaction was stopped 1 min later by the addition of 50 μL of ice-cold 6.6 N perchloric acid. Perchloric acid extracts were centrifuged at 11 000*g* for 5 min to eliminate protein precipitate, and cAMP was isolated from the supernatants using a mixture of trioctylamine and Freon (28/22, vol/vol). The upper aqueous phase was lyophilized, and the dry residue was dissolved in the buffer provided with the commercial radioimmunoassay kit for cAMP measurement.[4]

Potentiometric Studies and NMR Determinations. Potentiometric and NMR determinations were carried out as previously reported.[35,40] The experiments were performed in two steps in which 0.50 cm^3 of the same initial solution of compounds **1e** or **1a** of 5.0×10^{-3} mol dm^{-3} in ^2H_2O was successively subjected to potentiometric and NMR titrations. It should be noted that the glass electrode was calibrated in a concentration scale and the measurements done in ^2H_2O, so that here pH means the cologarithm of the concentration of $^2H^+$. The processing of the pH measurements allowed the total concentration of the ligand and the acid as well as the macroscopic protonation constants to be determined. One-dimensional ^{31}P NMR spectra were recorded at 121.50 MHz on a Bruker DPX-300 Fourier transform spectrometer. ^{31}P chemical shift values were referenced to an external 85% H_3PO_4 signal at 0.00 ppm with downfield shifts represented by positive values. Spectra were acquired over a spectral width of 10 ppm using a 0.1 s relaxation delay and a $\pi/2$ pulse. Typically, 1K data points were sampled with a corresponding 0.4 s acquisition time. Data were zero-filled and a 1 Hz exponential line broadening function was applied prior to Fourier transformation. The spectra had a digital resolution of 1.19 Hz per point. The HypNMR program[59] was used to check the potentiometrically determined protonation constants. The ^{1}H NMR titration was performed on the same equipment as before operating at 300.13 MHz. Spectra were acquired with water presaturation over a spectral width of 6 ppm using a 3 s relaxation delay and a $\pi/2$ pulse. With a corresponding 1.14 s acquisition time, 4K data points were sampled . The spectra had a digital resolution of 0.44 Hz per point. The temperature was controlled at 310 ± 0.5 K. The proton and phosphorus resonances were assigned by performing proton−proton and phosphorus−proton 2D correlation experiments at pH, thus allowing the titration curves to be characterized.

References

(1) Ralevic, V.; Burnstock, G. Receptors for purines and pyrimidines. *Pharmacol. Rev.* **1998**, *50*, 413−492.

(2) Hollopeter, G.; Jantzen, H.-M.; Vicent, D.; Li, G.; England, L.; Ramakrishnan, V.; Yang, R.-B.; Nurden, P.; Nurden, A.; Julius, D.; Conley, P. B. Identification of the platelet ADP receptor targeted by antithrombotic drugs. *Nature* **2001**, *409*, 202−207.

(3) Gachet, C. ADP Receptors of platelets and their inhibition. *Thromb. Haemostasis* **2001**, *86*, 222−232.

(4) Hechler, B.; Leon, C.; Vial, C.; Vigne, P.; Frelin, C.; Cazenave, J. P.; Gachet, C. The $P2Y_1$ receptor is necessary for adenosine 5′-diphosphate-induced platelet aggregation. *Blood* **1998**, *92*, 152−159.

(5) Léon, C.; Hechler, B.; Freund, M.; Eckly, A.; Vial, C.; Ohlmann, P.; Dierich, A.; LeMeur, M.; Cazenave, J.-P.; Gachet, C. Defective platelet aggregation and increased resistance to thrombosis in purinergic $P2Y_1$ receptor-null mice. *J. Clin. Invest.* **1994**, *104*, 1731−1737.

(6) Fabre, J.-E.; Nguyen, M.; Latour, A.; Keifer, J. A.; Audoly, L. P.; Coffman, T. M.; Koller B. H. Decreased platelet aggregation, increased bleeding time and resistance to thromboembolism in $P2Y_1$-deficient mice. *Nat. Med.* **1999**, *5*, 1199−1202.

(7) Léon, C.; Freund, M.; Ravanat, C.; Baurand, A.; Cazenave, J.-P.; Gachet, C. Key role of the $P2Y_1$ receptor in tissue factor-induced thrombin-dependent acute thromboembolism studies in $P2Y_1$−Knockout mice and mice treated with a $P2Y_1$ antagonist. *Circulation* **2001**, *103*, 718−723.
(8) Baurand, A.; Raboisson, P.; Freund, M.; Léon, C.; Cazenave, J. P.; Bourguignon, J. J.; Gachet, C. Inhibition of platelet function by administration of MRS2179, a $P2Y_1$ receptor antagonist. *Eur. J. Pharmacol.* **2001**, *412*, 213−221.
(9) Boyer, J. L.; Mohanram, A.; Gamaioni, E.; Jacobson, K. A.; Harden, T. K. Competitive and selective antagonism of $P2Y_1$ receptors by N^6-methyl-2′-deoxyadenosine-3′,5′-bisphosphate. *Br. J. Pharmacol.* **1998**, *124*, 1−3.
(10) Boyer, J. L.; Lazarowski, E.; Chen, X.-H.; Harden, T. K. Identification of a P2Y-purinergic receptor that inhibits adenylyl cyclase but does not activate phospholipase C. *J. Pharmacol. Exp. Ther.* **1993**, *267*, 1140−1146.
(11) Boyer, J. L.; Mohanram, A.; Deleney, S.; Waldo, G.; Harden, T. K. Signaling mechanism and pharmacological selectivity of an avian P2 receptor. Nucleotides and Their Receptors in the Nervous System, Leipzig, Germany, Aug 1, 1998; Abstract A03.
(12) Brown, S.; King, B. F.; Kim, Y.-C.; Burnstock, G.; Jacobson, K. A. Activity of novel adenine nucleotide derivatives as agonists and antagonists at recombinant rat P2X receptors. *Drug Dev. Res.* **2000**, *49*, 253−259.
(13) Camaioni, E.; Boyer, J. L.; Mohanram, A.; Harden, T. K.; Jacobson, K. A. Deoxyadenosine bisphosphate derivatives as potent antagonists at $P2Y_1$ receptors. *J. Med. Chem.* **1998**, *41*, 183−190.
(14) Fischer, B.; Boyer, J. L.; Hoyle, C. H. V.; Ziganshin, A. U.; Brizzolara, A. L.; Knight, G. E.; Zimmet, J.; Burnstock, G.; Harden, T. K.; Jacobson, K. A. Identification of potent, selective P2Y-purinoceptor agonists-structure−activity-relationships for 2-thioether derivatives of adenosine 5′-triphosphate. *J. Med. Chem.* **1993**, *36*, 3937−3946.
(15) Kim, Y.-C.; Gallo-Rodriguez, C.; Jang, S.-Y.; Nandanan, E.; Adams, M.; Harden, T. K.; Boyer, J. L.; Jacobson, K. A. Acyclic analogues of deoxyadenosine-3′,5′-bisphosphates as $P2Y_1$ receptor antagonists. *J. Med. Chem.* **2000**, *43*, 746−755.
(16) Nandanan, E.; Jang, S.-Y.; Moro, S.; Kim, H. O.; Siddiqui, M. A.; Russ, P.; Marquez, V. E.; Busson, R.; Herdewijn, P.; Harden, T. K.; Boyer, J. L.; Jacobson, K. A. Synthesis, biological activity, and molecular modeling of ribose-modified deoxyadenosine bisphosphate analogues as $P2Y_1$ receptor ligands. *J. Med. Chem.* **2000**, *43*, 829−842.
(17) Barrio, J. R.; Secrist, J. A., III; Leonard, N. J. Fluorescent adenosine and cytidine derrivatives. *Biochem. Biophys. Res. Commun.* **1972**, *46*, 597−604.
(18) Tsou, K. C.; Yip, K. F.; Miller, E. E.; Lo, K. W. Synthesis of 1,N^6-etheno-2-aza-adenosine (2-aza-∈-adenosine): a new cytotoxic fluorescent nucleoside. *Nucleic Acids Res.* **1974**, *1*, 531−547.
(19) Sako, M.; Hayashi, T.; Hirota, K.; Maki, Y. A newly devised method for the oxidative unmasking of 1,N^6-ethenoadenosine: facile conversion of adenosine into 2-deuterated adenosine. *Chem. Pharm. Bull.* **1992**, *40*, 1656−1658.
(20) Barlett, R. K.; Humphrey, I. R. Transamination of *N*,*N*-dimethylformamideazine. *J. Chem. Soc.* **1967**, *17*, 1664−1666.
(21) Samano, V.; Miles, R. W.; Robins, M. J. Efficient conversion of 6-aminopurines and nucleosides into 6-substituted analogues via novel 6-(1,2,4-triazol-4-yl)purine derivatives. *J. Am. Chem. Soc.* **1994**, *116*, 9331−9332.
(22) Vacca, J. P.; deSolms, S. J.; Huff, J. R. Total synthesis of D- and L-*myo*-inositol 1,4,5-trisphosphate. *J. Am. Chem. Soc.* **1987**, *109*, 3478−3479.
(23) Yu, K.-L.; Fraser-Reid, B. A novel reagent for the synthesis of myo-inositol phosphates: *N*,*N*-diisopropyl dibenzyl phosphoramidine. *Tetrahedron Lett.* **1988**, *29*, 979−982.
(24) Ti, G. S.; Gaffney, B. L.; Jones, R. A. Transient protection: efficient one-flask syntheses of protected deoxynucleosides. *J. Am. Chem. Soc.* **1982**, *104*, 1316−1319.
(25) Taunton-Rigby, A.; Kim, Y.-H.; Crosscup, C. J.; Starkovsky, N. A. Oligonucleoside synthesis. II. The Use of substituted trityl groups. *J. Org. Chem.* **1972**, *37*, 956−964.
(26) Humphries, R. G. Pharmacology of AR-C69931MX and related compounds: from pharmacological tools to clinical trials. *Haematologica* **2000**, *85*, 66−72.
(27) Martell, A. E.; Motekaitis, R. J. *Determination and Use of Stability Constants*, 2nd ed.; VCH Publishers: New York, 1992.
(28) Sarneski, J. E.; Reilley, C. N. The determination of proton-binding sites by "nmr titrations". In *Essays on Analytical Chemistry*; Wänninen, E., Ed.; Pergamon Press: Oxford, 1977; pp 35−49.
(29) Felemez, M.; Bernard, P.; Schlewer, G.; Spiess, B. Inframolecular protonation process of *myo*-inositol 1,4,5-tris(phosphate) and related compounds: Dynamics of the intramolecular interactions and evidence of C−H···O hydrogen bending. *J. Am. Chem. Soc.* **2000**, *122*, 3156−3165.
(30) Felemez, M.; Marwood, R. D.; Potter, B. V. L.; Spiess, B. Inframolecular studies of the protonation of adenophostin A: Comparison with 1-D-*myo*-inositol 1,4,5-trisphosphate. *Biochem. Biophys. Res. Commun.* **1999**, *266*, 334−340.
(31) Guédat, P.; Schlewer, G.; Kremp, E.; Riley, A. M.; Potter, B. V. L.; Spiess, B. Investigation of the inframolecular acid−base properties of D-*myo*-inositol 1,3,4,5-tetrakisphosphate and DL-*myo*-inositol 1,2,4,5-tetrakisphosphate. *J. Chem. Soc., Chem. Commun.* **1997**, 625−626.
(32) Liu, C. S.; Davis, R. J.; Nahorski, S. R.; Ballereau, S.; Spiess, B.; Potter, B. V. L. Synthesis, calcium mobilizing, and physicochemical properties of D-*chiro*-inositol 1,3,4,6-tetrakisphosphate, a novel and potent ligand at the D-*myo*-inositol 1,4,5-trisphosphate receptor. *J. Med. Chem.* **1999**, *42*, 1991−1998.
(33) Mernissi-Arifi, K.; Ballereau, S.; Schlewer, G.; Spiess, B.; Zenkouar, M. Microscopic acid−base properties of D-*myo*-inositol 1,2,6-tris(phosphate) and its 3,4,5-trideoxy analogue—influence of the hydroxy groups of the *myo*-inositol ring. *New J. Chem.* **1996**, *20*, 1087−1092.
(34) Mernissi-Arifi, K.; Schlewer, G.; Spiess, B. Inframolecular acid−base properties of *myo*-inositol 1,2,6-trisphosphate analogues—influence of the hydroxyl groups, phosphate configuration and intracyclic atom substitution. *Carbohydr. Res.* **1998**, *308*, 9−17.
(35) Mernissi-Arifi, K.; Schmitt, L.; Schlewer, G.; Spiess, B. Complete resolution of the microscopic: Protonation equilibria of D-*myo*-inositol 1,2,6-tris(phosphate) and related compounds by ^{31}P NMR and potentiometry. *Anal. Chem.* **1995**, *67*, 2567−2574.
(36) Rabenstein, D. L.; Sayer, T. L.; Determination of microscopic acid dissociation constants by nuclear magnetic resonance spectrometry. *Anal. Chem.* **1976**, *48*, 1141−1146.
(37) Riley, A. M.; Guedat, P.; Schlewer, G.; Spiess, B.; Potter, B. V. L. A conformationally restricted cyclic phosphate analogue of inositol trisphosphate—synthesis and physicochemical properties. *J. Org. Chem.* **1998**, *63*, 295−305.
(38) Sayer, T. L.; Rabenstein, D. L. Nuclear magnetic resonance studies of the acid−base chemistry of amino acids and peptides. III. Determination of the microscopic and macroscopic acid dissociation constants of α,ω-diaminocarboxylic acids. *Can. J. Chem.* **1976**, *54*, 3392−3400.
(39) Schlewer, G.; Guedat, P.; Ballereau, S.; Schmitt, L.; Spiess, B. Inositol phosphates: inframolecular physicochemical studies, correlation with binding properties. In *Phosphoinositides*: *Chemistry, Biochemistry, and Biomedical Applications*; Bruzik, K. S., Ed.; American Chemical Society: Washington, DC; pp 255−270.
(40) Schmitt, L.; Bortmann, P.; Schlewer, G.; Spiess, B. *Myo*-inositol 1,4,5-trisphosphate and related compounds' protonation sequence: potentiometric and ^{31}P NMR studies. *J. Chem. Soc., Perkin Trans. 2* **1993**, 2257−2263.
(41) Schweizer, M. P.; Broom, A. D.; Ts'o, P. O. P.; Hollis, D. P. Studies of inter- and intramolecular interaction in mononucleotides by proton magnetic resonance. *J. Am. Chem. Soc.* **1968**, *90*, 1042−1055.
(42) Martin, R. B. Nucleoside sites for transition metal ion binding. *Acc. Chem. Res.* **1985**, *18*, 32−38.
(43) Blindauer, C. A.; Holy, A.; Dvorakova, H.; Sigel, H. Solution properties of antiviral adenine-nucleotide analogues—the acid−base properties of 9-[2-(phosphonomethoxy)ethyl]adenine (pmea) and of its n1, n3 and n7 deaza derivatives in aqueous solution. *J. Chem. Soc., Perkin Trans. 2* **1997**, 2353−2363.
(44) Tribolet, R.; Sigel, H. Self-association and protonation of adenosine 5′-monophosphate in comparison with its 2′- and 3′-analogues and tubericin 5′-monophosphate (7-deaza-AMP). *Eur. J. Biochem.* **1987**, *163*, 353−363.
(45) Wang, X.; Simpson, J. H.; Nelson, D. J. ^1H and ^{31}P NMR study of speciation in systems containing ADP, Al^{3+}, and fluoride. *J. Inorg. Biochem.* **1995**, *58*, 29−47.
(46) White, A. M.; Varney, M. A.; Watson, S. P.; Rigby, S.; Changsheng, L.; Ward, J. G.; Reese, C. B.; Graham, H. C.; Williams, R. J. P. Influence of Mg^{2+} and pH on nmr spectra and radioligand binding of inositol 1,4,5-trisphosphate. *Biochem. J.* **1991**, *278*, 759−764.
(47) Halbfinger, E.; Major, D. T.; Ritzmann, M.; Ubl, J.; Reiser, G.; Boyer, J. L.; Harden, K. T.; Fischer, B. Molecular recognition of modified adenine nucleotides by the P2Y(1)-receptor. 1. A synthetic, biochemical, and NMR approach. *J. Med. Chem.* **1999**, *42*, 5325−5337.
(48) Thibaudeau, C.; Plavec, J.; Chattopadhyaya, J. Quantitation of the anomeric effect in adenosine and guanosine by comparison of the thermodynamics of the pseudorotational equilibrium of the pentofuranose moiety in N- and C-nucleosides. *J. Am. Chem. Soc.* **1994**, *116*, 8033−8037.
(49) Plavec, J.; Garg, N.; Chattopadhyaya, J. How does the steric effect drive the sugar conformation in the 3′-C-branched nucleosides? *J. Chem. Soc., Chem. Commun.* **1993**, 1011−1014.

(50) Thibaudeau, C.; Plavec, J.; Watanabe, K. A.; Chattopadhyaya, J. How do the aglycones drive the pseudorotational equilibrium of the pentofuranose moiety in C-nucleosides? *J. Chem. Soc., Chem. Commun.* **1994**, 537−540.
(51) Plavec, J.; Thibaudeau, C.; Viwanadham, G.; Sund, C.; Chattopadhyaya, J. How does the 3′-phosphate drive the sugar conformation in DNA? *J. Chem. Soc., Chem. Commun.* **1994**, 781−783.
(52) Haasnoot, C. A. G.; De Leeuw, F. A. A. M.; Altona, C. The relation between proton−proton NMR coupling constants and substituent electronegativities. I. An empirical generalization of the Karplus equation. *Tetrahedron* **1980**, *36*, 2783−2792.
(53) Beevers, A. P. G.; Witch, E. M.; Jones, B. C. N. M.; Cosstick, R.; Arnold, J. R. P.; Fisher, J. Conformational analysis of 3′-S-PO_3-linked ribo- and deoxyribodinucleoside monophosphates. *Magn. Reson. Chem.* **1999**, *37*, 814−820.
(54) Altona, C.; Sundaralingam, M. Conformational analysis of the sugar ring in nucleosides. Improved for the interpretation of proton magnetic resonance coupling constants. *J. Am. Chem. Soc.* **1973**, *95*, 2333−2344.
(55) Hotoda, H.; Murayama, K.; Miyamoto, S.; Iwata, Y.; Takahashi, M.; Kawase, Y.; Tanzawa, K.; Kaneko, M. Molecular recognition of adenophostin, a very potent Ca^{2+} inducer, at the D-myoinositol 1,4,5-trisphosphate receptor. *Biochemistry* **1999**, *38*, 9234−9241.
(56) Plavec, J.; Thibaudeau, C.; Chattopadhyaya, J. How does the 2′-hydroxy group drive the pseudorotational equilibrium in nucleoside by the tuning of the 3′-gauche effect? *J. Am. Chem. Soc.* **1994**, *116*, 6558−6560.
(57) Hofmann, M.; Adeco, M.; Fagan, P.; Wemmer, D.; Eritja, R.; Diaz, A. R. Synthesis of oligodeoxynucleotides containing N6-[13C-methyl]adenine and N2-[13C-methyl]guanine. *J. Chem. Soc., Perkin Trans. 1* **1997**, *12*, 1825−1828.
(58) Cazenave, J. P.; Hemmendinger, S.; Beretz, A.; Sutter-Bay, A.; Launay, J. L'agrégation plaquettaire: outil d'investigation clinique et d'étude pharmacologiques-methodologie. *Ann. Biol. Clin.* **1983**, *41*, 167−179.
(59) Frassineti, C.; Ghelli, S.; Gans, P.; Sabatini, A.; Moruzzi, M. S.; Vacca, A. Nuclear magnetic resonance as a tool for determining protonation constants of natural polyprotic bases in solution. *Anal. Biochem.* **1995**, *231*, 374−382.

JM0104062